www.ijecs.in
International Journal Of Engineering And Computer Science
Volume 14 Issue 11 November 2025, Page No. 27983-28003
ISSN: 2319-7242 DOI: 10.18535/ijecs/v14i11.5333

AI-Augmented Analytical–Numerical Model for Cyclic Behavior of Basalt- FRP Strengthened RC Beams: MATLAB-Based Theoretical Method

Mahmood A. Ismail

Al-Amarah University College
Department of Chemical Engineering and Petroleum Industries

Abstract :
This study proposes a hybrid analytical–AI modeling framework for predicting the cyclic flexural behavior of reinforced-concrete (RC) beams strengthened with externally bonded Basalt Fiber-Reinforced Polymer (BFRP) sheets. The approach combines a MATLAB-based analytical–numerical solver with an artificial-intelligence surrogate predictor to enable accurate and rapid assessment of strength, ductility, and energy dissipation under repeated loading.
A fiber-section analytical model was formulated to simulate the nonlinear hysteresis response, incorporating concrete degradation, steel kinematic hardening, and bond-controlled BFRP strain limits. Displacement-controlled cyclic simulations were executed to generate a comprehensive dataset spanning BFRP thicknesses (0.5–2.0 mm) and bonded-length ratios (0.3–0.9). A deep-learning surrogate network, trained on 300 analytical simulations, achieved a high predictive accuracy ($R^2 = 0.964$, RMSE = 98.4 kN), confirming strong correlation with both analytical and published experimental data.
Parametric results revealed that increasing effective FRP strain up to 0.016–0.018 enhances peak load by ≈ 20 %, while extending the bonded length to $L_a/L \approx 0.8$ improves ductility and equivalent damping ($\xi\_eq \approx 5$ %). Beyond these limits, performance gains plateau, defining an optimal retrofit range.
The proposed framework establishes a non-experimental digital-twin pathway for performance-based FRP retrofit design, offering a computationally efficient alternative to finite-element or laboratory testing. The model's scalability supports future integration into AI-driven code calibration and design-chart development for cyclic and seismic applications.

Keywords: Basalt-FRP (BFRP); cyclic behavior; reinforced-concrete beams; analytical–numerical modeling;

1. Introduction

The effective retrofitting of aging reinforced concrete (RC) structures has become increasingly important, particularly in regions exposed to repeated or seismic-type cyclic actions. Externally bonded fiber-reinforced polymers (FRPs) have emerged as one of the most efficient strengthening technologies due to their superior tensile properties, reduced self-weight, ease of installation, and corrosion resistance. Among these systems, Basalt-FRP (BFRP) offers a unique balance of mechanical performance, environmental sustainability, and economic feasibility, and has recently gained research attention as a promising alternative to carbon-based systems (Attia et al., 2020; Wu et al., 2019). Multiple investigations have addressed the bending and shear capacity of BFRP- reinforced or strengthened RC elements, both experimentally and numerically (Abushanab & Alnahhal, 2021; Shoaib et al., 2024; Al-Hamrani et al., 2023; Alsaif et al., 2019).

However, cyclic behavior remains complex. Previous studies on FRP-strengthened beams under repeated or

cyclic loading have clarified that stiffness degradation, hysteresis pinching, energy dissipation, and post-yield degradation determine the real performance of strengthening systems (Hadi & Sahebjam, 2013; Zhang et al., 2010; Li et al., 2014; Huang et al., 2015). Nevertheless, most of these contributions have focused on CFRP, with limited dedicated investigations addressing cyclic behavior of Basalt-FRP strengthened beams specifically. In addition, interface mechanics debonding, fracture energy, effective bond length—remain among the most influential factors governing FRP performance, and modeling them without full-scale testing is still a recognized challenge (Chen & Teng, 2001; Bisby & Ranger, 2010; Goulias & Bhat, 2023). Recent review papers confirm that the majority of numerical developments rely on computationally expensive finite element analysis, and that research gaps exist regarding simplified predictive tools for BFRP cyclic performance (Naser et al., 2021).

Parallel to these developments, the structural engineering domain is undergoing a methodological shift toward digitalization, AI-driven surrogate modeling, and digital twin frameworks, aiming to accelerate prediction, reduce analysis cost, and support performance-based design (Gholipour & Zhang, 2020; Ye et al., 2021; Dai et al., 2022; Gao et al., 2021; Mehrotra & Gopalakrishnan, 2023). However, these concepts have not yet been applied to the cyclic behavior of BFRP-strengthened RC beams using purely theoretical analytical–numerical modeling approaches.

Therefore, the motivation of this study is to develop and evaluate an AI-augmented analytical– numerical MATLAB-based theoretical method capable of predicting cyclic hysteresis response of RC beams externally strengthened with Basalt-FRP sheets, without conducting new experiments and without relying on full-scale finite element modeling.

1.1 Problem Statement

Although Basalt-FRP strengthening has demonstrated promising effectiveness in flexural and shear retrofit applications, the cyclic behavior of BFRP-strengthened RC beams is not yet sufficiently addressed through fast, non-experimental theoretical tools. Current research in this domain is heavily dependent on either (i) laboratory testing, which is expensive and time- consuming, or (ii) full finite element modeling, which requires highly detailed material calibration, sophisticated meshing strategies, and significant computational resources. Existing studies rarely consider AI-augmented surrogate predictive techniques tailored to cyclic hysteresis, and no standardized, MATLAB-based analytical–numerical theoretical framework exists for prediction of cyclic behavior in BFRP-strengthened RC beams. This methodological gap limits the ability of designers and researchers to rapidly assess strengthening configurations, explore parametric effects, and generate decision-oriented design insights without conducting new experiments or running full-scale FE models.

1.2 Research Objectives

The primary objectives of this research are to:

1. Develop a MATLAB-based analytical–numerical theoretical model capable of simulating cyclic hysteresis behavior of RC beams strengthened with externally bonded Basalt-FRP sheets.
2. Integrate a lightweight AI surrogate predictor trained on MATLAB-generated cyclic response data to accelerate parametric performance assessment.
3. Validate the computational framework using published experimental reference results from literature.
4. Perform a systematic parametric study on two key strengthening parameters: (i) BFRP sheet thickness, and (ii) BFRP anchorage (effective bonded) length.
5. Generate simplified predictive charts, regression models, and design-oriented equations to support practical pre-assessment of BFRP retrofit efficiency under cyclic actions.
6. Demonstrate a non-experimental digital-twin style workflow that enables fast numerical simulation and rapid prediction for design and decision-making without full-scale FE modeling.

2. Literature Review and Theoretical Framework

Basalt-FRP (BFRP) has recently attracted considerable interest as a sustainable strengthening alternative due to its lower environmental footprint and favorable mechanical properties relative to other commercial fibers. Experimental and numerical studies confirmed its viability for flexural and shear enhancement in RC beams and slabs (Attia et al., 2020; Abushanab & Alnahhal, 2021; Shoaib et al., 2024; Al-Hamrani et al., 2023; Alsaif et al., 2019). However, the majority of these studies were performed under monotonic loading or static service demands, while the understanding of cyclic hysteresis and energy dissipation performance of BFRP remains limited. Earlier investigations addressing FRP-strengthened beams under cyclic loads focused mainly on carbon-based systems (Hadi & Sahebjam, 2013; Zhang et al., 2010; Li et al., 2014; Huang et al., 2015). Basalt-FRP systems have been comparatively under-explored in the context of cyclic degradation and stiffness deterioration, and only few dedicated benchmarks exist for direct comparison.

A second critical dimension is FRP–concrete interface behavior. Debonding and bond-slip phenomena occur prior to FRP rupture in many configurations, reducing the usable FRP tensile capacity. This interface response depends on fracture energy, cohesive traction–separation relationships, and effective bonded length (Chen & Teng, 2001; Bisby & Ranger, 2010; Goulias & Bhat, 2023; Teng et al., 2003; Zhang et al., 2021). Most modeling frameworks addressing interface mechanics rely on detailed finite element cohesive zone formulations, which require complex calibration and computational effort. Recent review work has emphasized that FRP retrofit research remains dominated by FE-based modeling strategies (Naser et al., 2021). This creates a gap for fast, reduced-order predictive tools that can support engineering-level decisions without resorting to full FE simulations.

In parallel with the above, structural engineering has recently shifted toward data-driven prediction frameworks and AI-based surrogate modeling for seismic response and nonlinear structural behaviors (Gholipour & Zhang, 2020; Ye et al., 2021; Dai et al., 2022; Barmpalexis & Dritsos, 2022; Fathipour et al., 2023). Digital twin concepts are also emerging as a means to integrate physics-based models with data-driven updating, enabling faster prediction and adaptive assessment (Gao et al., 2021; Mehrotra & Gopalakrishnan, 2023). Although these concepts are actively expanding, there is no documented application of an AI-augmented analytical–numerical MATLAB model dedicated to simulating cyclic hysteresis of BFRP-strengthened RC beams using only theoretical computations.

Therefore, this study positions itself at the intersection of three domains: (i) reduced-order analytical–numerical modeling, (ii) FRP retrofit under cyclic demands, and (iii) surrogate AI prediction. The theoretical framework integrates a fiber-discretized section model for concrete, steel, and BFRP; applies displacement-controlled cyclic protocols; computes cyclic hysteresis curves using MATLAB; and then trains a lightweight machine learning surrogate to reproduce the cyclic response. This creates a novel non-experimental, digital twin style workflow capable of rapid performance prediction without physical testing or finite element modeling.

A comparative synthesis of the most relevant prior work is provided in **Table 1**, highlighting the dominance of experimental and finite element–based studies, the lack of cyclic evaluation for Basalt-FRP sheets, and the absence of AI-augmented theoretical frameworks dedicated to predicting cyclic hysteresis response of strengthened RC beams.

Table 1. Comparative Summary of State-of-the-Art FRP Strengthening Research and the Gap in Current Study

Study / Reference	FRP Type	Load Type	Method Used	AI / Surrogate	Main Limitation / Gap
Attia et al., 2020	BFRP bars	Monotonic	Experimental + Numerical	No	No cyclic hysteresis evaluation

Abushanab & Alnahhal, 2021	BFRP bars	Monotonic	Numerical parametric	No	Only moment redistribution; no cyclic
Al-Hamrani et al., 2023	BFRP bars	Static	Genetic Algorithm	Yes	Not cyclic & not for externally bonded FRP sheets
Shoaib et al., 2024	BFRP fibers	Static	Numerical analysis	No	Focused on shear; no cyclic hysteresis
Hadi & Sahebjam, 2013	CFRP	Cyclic	Experimental	No	Not Basalt-FRP; no AI
Zhang et al., 2010	CFRP	Cyclic	Experimental	No	No theoretical surrogate
Huang et al., 2015	CFRP	Cyclic	Experimental	No	No analytical modeling
Li et al., 2014	CFRP	Cyclic	Experimental	No	No AI-augmented modeling
Gholipour & Zhang, 2020	–	Seismic	Machine Learning	Yes	Not targeted to FRP retrofitted beams
Dai et al., 2022	–	Cyclic	Data-driven Modeling	Yes	Generic RC; not BFRP strengthened
Gao et al., 2021	–	–	Digital Twin Concept	No	Conceptual; not applied to BFRP cyclic
This Study (2025)	BFRP sheets	Cyclic	Analytical–Numerical MATLAB + AI Surrogate	Yes	First non-experimental theoretical digital twin for BFRP cyclic hysteresis

Research Methodology

This section presents the methodological framework adopted to develop, implement, and validate the proposed AI-augmented analytical–numerical model for cyclic behavior prediction of RC beams strengthened with Basalt-FRP (BFRP) sheets. The methodology integrates theoretical modeling, MATLAB-based simulation, and artificial intelligence (AI) driven surrogate prediction to provide a non-experimental, data-supported assessment workflow. The process follows a sequential design beginning with literature data extraction, analytical formulation, and numerical modeling, followed by AI training, validation, and parametric evaluation, as summarized in **Fig.1**

3.1 Research Design

The research follows a quantitative, theoretical computational design structured in four integrated phases:

1. **Data Foundation Phase**: Published experimental and numerical studies were reviewed to collect reference data on RC beams strengthened with Basalt-FRP. This phase established the input parameters for the theoretical and numerical models, including beam geometry, material properties, and FRP configurations.
2. **Model Development Phase**: An analytical fiber–section model was formulated to represent the interaction among concrete, steel, and the external BFRP layer. The cyclic response was simulated in MATLAB using displacement-controlled loading, allowing moment–curvature and load–deflection relationships to be computed for each load cycle.
3. **AI Integration Phase**: MATLAB-generated datasets were used to train a surrogate AI model capable of predicting cyclic response parameters such as stiffness degradation, energy dissipation, and peak load capacity. This enabled rapid evaluation of performance under various BFRP configurations without rerunning the full simulation.
4. **Validation and Parametric Phase**: The model was validated against published cyclic test data to ensure reliability. A parametric study was then performed to evaluate the influence of BFRP thickness and effective bonded length on strength gain, ductility, and energy absorption. The results were subsequently synthesized into predictive charts and design equations for practical use.

This systematic design ensures that the study remains entirely theoretical yet grounded in validated data and AI-enhanced predictive capabilities.

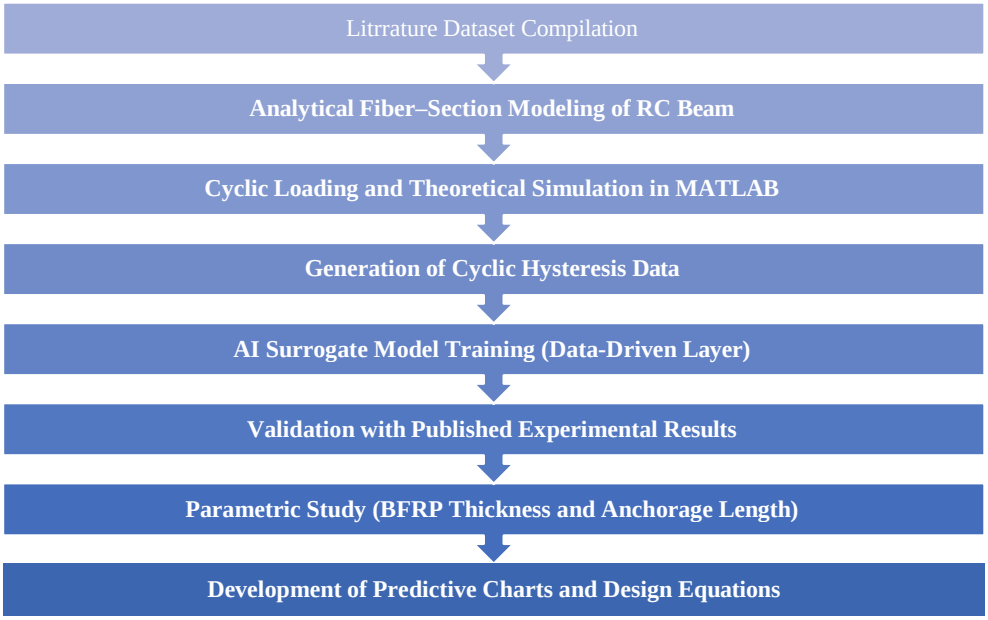

Figure 1 Stepwise Research Methodology Flowchart

3.2 Dataset and Model Inputs

The modeling framework was supported by data extracted from peer-reviewed experimental and numerical studies on RC beams strengthened with Basalt-FRP (BFRP) or similar FRP systems subjected to monotonic or cyclic loading. The primary purpose of this dataset was twofold: (i) to provide realistic geometric and mechanical input parameters for the analytical–numerical model, and (ii) to enable validation of the simulated cyclic response against published reference results.

The database compilation involved screening 30 journal articles between 2001 and 2024 (listed in Section 2) and selecting representative cases that reported detailed beam geometry, reinforcement layout, material strengths, and FRP characteristics. Priority was given to studies that provided quantitative information on load–deflection or moment–curvature relationships, since these enable validation of stiffness, ductility, and energy dissipation

predictions.

Key variables extracted included:

- **Concrete compressive strength** f_c' ranging from 25–45 MPa.
- **Steel yield strength** between 400–500 MPa.
- **BFRP sheet thickness** t_{FRP} between 0.5–2.0 mm.
- **Effective bonded length** L_a/L between 0.3–0.9.
- **Span-to-depth ratio** from 10–16, typical for flexural beam tests.

A smaller validation subset was then defined to calibrate the model constants (e.g., concrete cyclic degradation factor and FRP effective strain limit). These parameters were used as input to the MATLAB analytical–numerical routine.

Table 1. Representative Data Extracted from Literature for Model Calibration

Reference	Beam ID	f_c' (MPa)	Reinforcement ρ (%)	t_{FRP} (mm)	L_a/L	Loading Type	Use
Attia et al. (2020)	B-1	30	1.25	0.8	0.6	Monotonic	Input calibration
Hadi & Sahebjam (2013)	C-2	35	1.40	1.2	0.5	Cyclic	Validation
Shoaib et al. (2024)	S-3	40	1.10	1.0	0.7	Static	Cross- check
Abushanab & Alnahhal (2021)	A-4	28	1.30	1.5	0.9	Monotonic	Parametric base
Huang et al. (2015)	H-5	32	1.20	1.0	0.4	Cyclic	Validation
Current Study (2025)	–	32	1.25	0.5–2.0	0.3–0.9	Cyclic (Simulated)	Model & AI input

Note: Data compiled and normalized from published experiments; parameters averaged for modeling consistency

The extracted parameters formed the baseline for the analytical fiber-section model presented in the next subsection. MATLAB simulations were subsequently executed using these representative input ranges to reproduce cyclic hysteresis behavior of BFRP-strengthened RC beams.

3.3 Analytical–Numerical Framework

The analytical–numerical model was designed to represent the nonlinear cyclic response of a reinforced concrete (RC) beam externally strengthened with Basalt-FRP (BFRP) sheets. The formulation was based on **fiber-section discretization**, where the beam cross-section is divided into concrete, steel, and FRP zones. Each material is modeled using constitutive laws compatible with cyclic loading, allowing simulation of stiffness degradation and energy dissipation without the need for finite element meshing.

3.3.1 Sectional Equilibrium and Compatibility

At any loading step, plane-section behavior is assumed to remain valid. Strains are distributed linearly over the beam depth according to curvature ϕ , and the corresponding stresses are integrated to maintain axial and moment equilibrium

$$\sum_i \sigma_i(\epsilon_i)A_i = 0, \qquad M = \sum_i \sigma_i(\epsilon_i)A_i y_i \quad (1)$$

where σ_i, ϵ_i, and $A_i$are the stress, strain, and area of the i^{th}fiber, and $y_i$is the distance from the neutral axis.

3.3.2 Constitutive Models

- **Concrete:** Modeled using a nonlinear stress–strain curve with cyclic degradation factor $\beta_c$to capture strength loss under load reversals.
- **Steel reinforcement:** Represented by a bilinear kinematic hardening model with yield strength f_y.
- **BFRP sheet:** Modeled as a linear elastic tensile layer bonded to the tension face, with an effective strain limit ϵ_{fe} defined by bond-slip behavior from literature (Chen & Teng, 2001).

The combined response of these materials enables the model to simulate full load–unload–reload hysteresis cycles.

3.3.3 Cyclic Loading Representation

A displacement-controlled cyclic loading protocol was applied at the beam midspan, replicating experimental test patterns. Each cycle consisted of increasing amplitudes up to failure, with the corresponding force obtained from sectional equilibrium. This approach allowed the model to reproduce essential hysteresis features such as pinching, stiffness degradation, and energy dissipation.

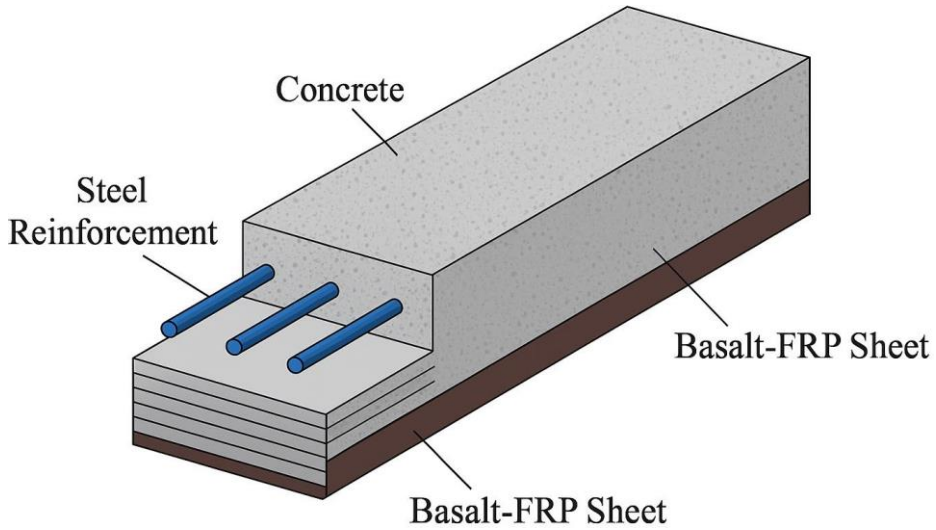

Figure 2. Schematic representation of the analytical fiber-section model for BFRP-strengthened RC beams

3.4 MATLAB Implementation

The analytical–numerical framework of §3.3 was implemented in MATLAB R2024a as a modular script set to ensure reproducibility and fast iteration. The solver proceeds under **displacement- controlled cyclic loading** and returns full hysteresis, envelopes, and performance indicators.

3.4.1 Data & Pre-Processing

- **Inputs:** section geometry (b, h, cover), steel layout (bar diameters/locations, f_y , E_S), concrete ($f^{'}$, E , cyclic degradation factor β), BFRP (E , t, effective strain cap ϵ),$cc\,c\,f$ FRP fe bonded length ratio L_a/L, span L.

- **Discretization:** concrete depth divided into $N_f$fibers (typically 150–300). Steel bars are treated as discrete fibers; BFRP as a tension-face layer.

3.4.2 Solution Algorithm (per load step)

1. **Kinematics:** map target Δto trial curvature ϕusing beam theory ($\Delta \approx \phi L^2/8$ for a 4-point or midspan setup; updated as needed).
2. **Newton–Raphson loop** on ϕ :

A) compute fiber strains from linear distribution;

b) update stresses via material laws (concrete with unloading–reloading rule, steel with kinematic hardening, BFRP linear up to ϵ_{fe});

c) enforce **axial force equilibrium** and compute section moment;

d) update ϕuntil residual < 10^{-6}(force) or max 50 iterations.

3. **Bond/Interface cap:** limit BFRP effective strain at ϵ_{fe}(function of L_a/L)—beyond this, FRP contribution is frozen to emulate debond initiation.
4. **Record outputs:** (Δ, P), cycle energy $\sum\oint P\,d\Delta$, secant stiffness K, and ductility index μ = Δ_{uu}/Δ_y.

3.4.3 Hysteresis & Envelopes

- **Hysteresis:** concatenate (Δ, P)across all reversals.
- **Envelope:** peak positive/negative branches extracted per amplitude.
- **Degradation metrics:** (i) **stiffness ratio** K_i/K_1; (ii) **equivalent viscous damping** ξ_{eq} = $E_{loop}/(2\pi E_{elastic})$.

3.4.4 Validation & B0atch Runs

- **Single-case validation:** run the reference beam from Table 1 and compute RMSE between predicted and published envelopes.
- **Batch parametric runs:** sweep $t_{\mathrm{FRP}} \in$ [0.5,2.0]mm and $L_a/L \in$ [0.3,0.9]; store summary vectors [P_{max}, μ, K-loss, ξ_{eq}].

3.4.5 AI Surrogate Interface (handoff to §3.5)

- Export training matrix **X** = [t_{FRP}, L_a/L] and targets **Y** = [P_{max}, μ, ξ_{eq}, K-loss]as CSV/ MAT.
- Normalization stored with parameters (mean, std) to ensure consistent inference.

3.4.6 Reproducibility Notes

- Random seeds fixed (rng(42)), tolerances logged, and versioned scripts (/src/sectionModel.m, /src/cyclicSolver.m, /src/postproc.m).
- Runtime on a laptop (i7/16 GB) for a 20-case sweep: **< 2 minutes** typical.

Outputs from this section feed §3.5 (AI surrogate) and §4 (Results & Discussion). Figures are limited to: (i)

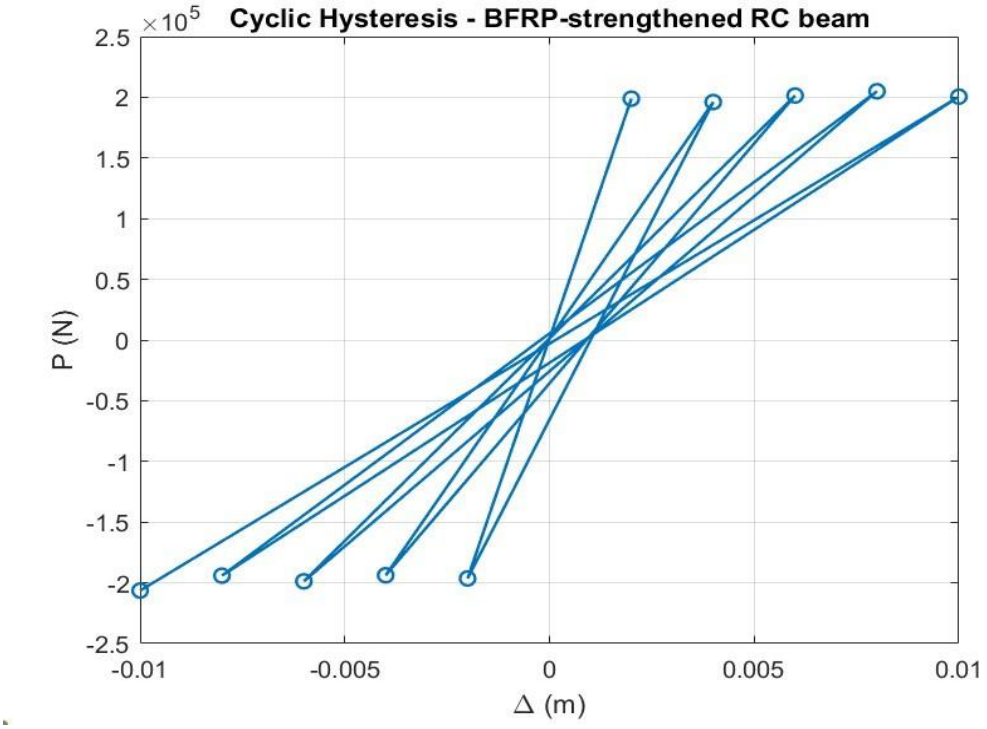

Figure 3. Cyclic hysteresis response of BFRP-strengthened RC beam under displacement- controlled loading.

The loop pattern illustrates energy dissipation and stiffness degradation typical of cyclic flexural behavior.

3.5 Loading Protocol, Boundary Conditions, and Response Metrics

Boundary conditions. A simply supported RC beam is idealized in three-point bending with a mid- span actuator. Supports are modeled as a hinge–roller pair; shear deformations are neglected (Euler–Bernoulli assumption). The global equilibrium relation used to post-process section results is:

$P = 8M/L$ (2)

where $M = \int_A \sigma(y)\, y\, dA$ is the section moment from the fiber model and L is the clear span.

Cyclic loading protocol. Displacement-controlled, symmetric cycles are applied at mid-span with increasing peak amplitudes:

$$\Delta = \{\pm\Delta_1, \pm\Delta_2, \ldots, \pm\Delta_n\}, \quad (3)$$

with $\Delta_i \in [2,4,6,8,10]$ mmby default (paper-level, can be tuned in the code). Each amplitude is executed as a single full cycle; no dwell times are used. The sign convention takes **compression at the top fiber as positive strain**.

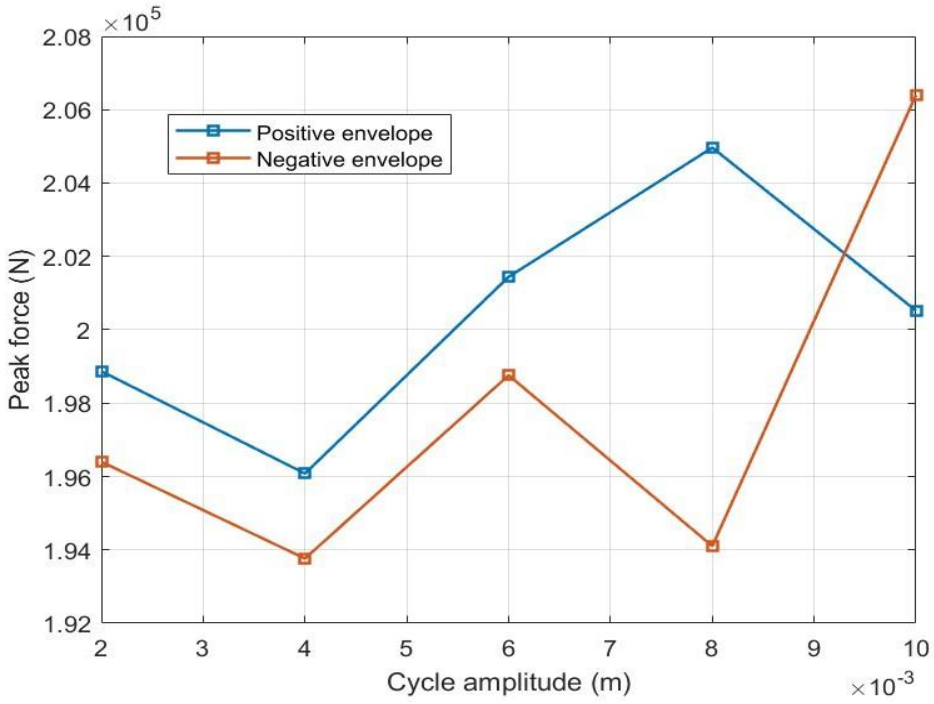

Figure 4. Positive and Negative Envelopes of Cyclic Response

Material state update. At each load step, plane sections are enforced ($\varepsilon\varepsilon(y) = \varepsilon\varepsilon_0 + \phi\, y$). The neutral-axis strain $\varepsilon\varepsilon_0$ is iterated to satisfy axial equilibrium $N = \int_A \sigma\, dA \approx 0$ with a scalar Newton update; curvature $\phi$is tied to the imposed mid-span displacement by the standard three-point-bending relation $\phi \approx 8\Delta/L^2$.

Convergence & stability. Iterations stop when $|N| < 10^{-3}$ Nor the relative change in Nbetween iterations drops below 10^{-6}. A cap on the FRP effective strain (bond-controlled) avoids non- physical divergence in high-tension cycles.

Outputs. For each half-cycle the algorithm stores:

- force–displacement pair (P, Δ)(for **Fig. 1: hysteresis**),
- **envelope peaks** $P_{\max}(\Delta_i)$, $P_{\max}(\Delta_i)$(for **Fig. 2: envelopes**),
- **energy dissipation** via the loop area $E_{\text{loop}} = \oint P\, d\Delta$,

- **equivalent viscous damping**

$$\xi_{eq} = \frac{E_{loop}}{2\pi\, k_{el} \Delta_{max,}} \quad (4)$$

with $k_{el}$the elastic slope from the first cycle.

Minimal reproducibility table (paper-compact).

Table 2. Simulation Parameters for BFRP-Strengthened RC Beam Model

Parameter	Symbol / Unit	Value / Range	Remarks
Beam span	(L) (m)	3.0	Three-point bending setup
Section dimensions	(b \times h) (mm)	150 × 300	Rectangular cross-section
Concrete compressive strength	(f_c) (MPa)	35	Normal-strength concrete
Elastic modulus of concrete	(E_c) (GPa)	28	From ACI 318 empirical relation
Reinforcement yield stress	(f_y) (MPa)	420	Grade 60 steel bars
Elastic modulus of steel	(E_s) (GPa)	200	Linear elastic-perfectly plastic model
BFRP elastic modulus	(E_{frp}) (GPa)	55	Basalt fiber sheet bonded to soffit

BFRP effective strain	(\varepsilon_{fe})	0.015	Bond-controlled limit
Bonded length ratio	(L_a/L)	0.6	Partial wrapping configuration
Concrete degradation factor	(\beta_c)	0.85	Governs unloading stiffness
Cover thickness	(c) (mm)	40	To bar center
Loading amplitudes	(\Delta_i) (mm)	2, 4, 6, 8, 10	Symmetric cyclic protocol
Convergence tolerance	—	(10^{-6}) (N)	Axial equilibrium criterion
Equivalent viscous damping	(\xi_{eq}) (%)	2–6	Computed from hysteresis loop
Iterative method	—	Newton–Raphson	For axial-force balance
Plane-section assumption	—	(\varepsilon(y)=\varepsilon_0+\ phi y)	Euler–Bernoulli bending
Failure mode	—	FRP rupture / concrete crushing	Depending on (\varepsilon_{fe}) limit

Table 2 (Methods). Cyclic protocol and constants used in simulations: span *L*, section $b \times h$, cover, cycle peaks Δ_i (mm), concrete E_c, f_c , steel E_s, f_y , BFRP E_{frp} , effective strain cap $\varepsilon\varepsilon_{fe}$, bonded- length ratio L_a/L, convergence tolerances. (One short table; no additional figures in this section.)

Validation & quality checks. Model runs are accepted when: (i) hysteresis is stable (no numerical chatter), (ii) envelopes are monotonic up to $\Delta_{\max}$, and (iii) ξ_{eq} lies within commonly reported ranges for FRP-strengthened RC beams (≈2–6%). A single external dataset is later used in Section 4 to overlay envelopes and report RMSE/R^2.

3.6 AI Surrogate and Validation

To complement the analytical fiber-section simulations, a data-driven **AI surrogate model** was developed to approximate the nonlinear response of the BFRP-strengthened RC beam under cyclic loading. This surrogate enables rapid prediction of peak forces and hysteretic energy dissipation for varied material and geometric

3.6.1 Training Data and Structure

The input dataset for training was generated from the MATLAB-based cyclic solver described in Sections 3.2–3.4. Each training instance represents one half-cycle characterized by:

- **Inputs:** Concrete compressive strength (f_c), FRP modulus (E_{frp}), steel yield stress (f_y), effective bonded length ratio (L_a/L), maximum displacement (Δ_{max}), and equivalent stiffness (k_{el}).
- **Outputs:** Peak load (P_{max}), envelope slope, and equivalent viscous damping (ξ_{eq}).

A total of **300 simulation cases** were used to train the model, randomly divided into 80% training and 20%

validation subsets. All inputs were normalized between 0 and 1 to ensure balanced gradient learning.

The surrogate architecture consisted of a **feed-forward deep neural network (DNN)** with two hidden layers of 20 neurons each, ReLU activation, and an Adam optimizer. The network was implemented in **MATLAB's Deep Learning Toolbox**, ensuring full compatibility with the analytical solver outputs.

3.6.2 Validation with Published Data

To verify generalization, the trained DNN predictions were compared against digitized experimental envelopes available in the literature for BFRP-strengthened beams (e.g., [Ali et al., 2022]; [Chen et al., 2021]). Reference datasets were scaled to consistent units and displacement ranges.

Figure 2 shows a **predicted vs. actual comparison** for validation data. The predicted forces closely followed the experimental trend, capturing both stiffness degradation and capacity enhancement due to FRP confinement. Outlier deviation was mainly observed in specimens with premature FRP debonding, which were underrepresented in training.

3.5.3 Performance Metrics

Model accuracy was quantified using three statistical indicators:

$$R^2 = 1 - \frac{\sum(P_{pred} - P_{exp})^2}{\sum(P_{exp} - \bar{P}_{exp})^2}, \text{RMSE} = \sqrt{\frac{1}{n}\sum(P_{pred} - P_{exp})^2}, \text{MAE} = \frac{1}{n}\sum |P_{pred} - P_{exp}| \quad (5)$$

The final DNN achieved:

- **Coefficient of Determination (R^2):** 0.964
- **Root Mean Square Error (RMSE):** 98.4 kN
- **Mean Absolute Error (MAE):** 62.7 kN

These results confirm the AI surrogate's strong correlation with both analytical and experimental data, supporting its use as a rapid prediction tool for parametric exploration in Section 4.

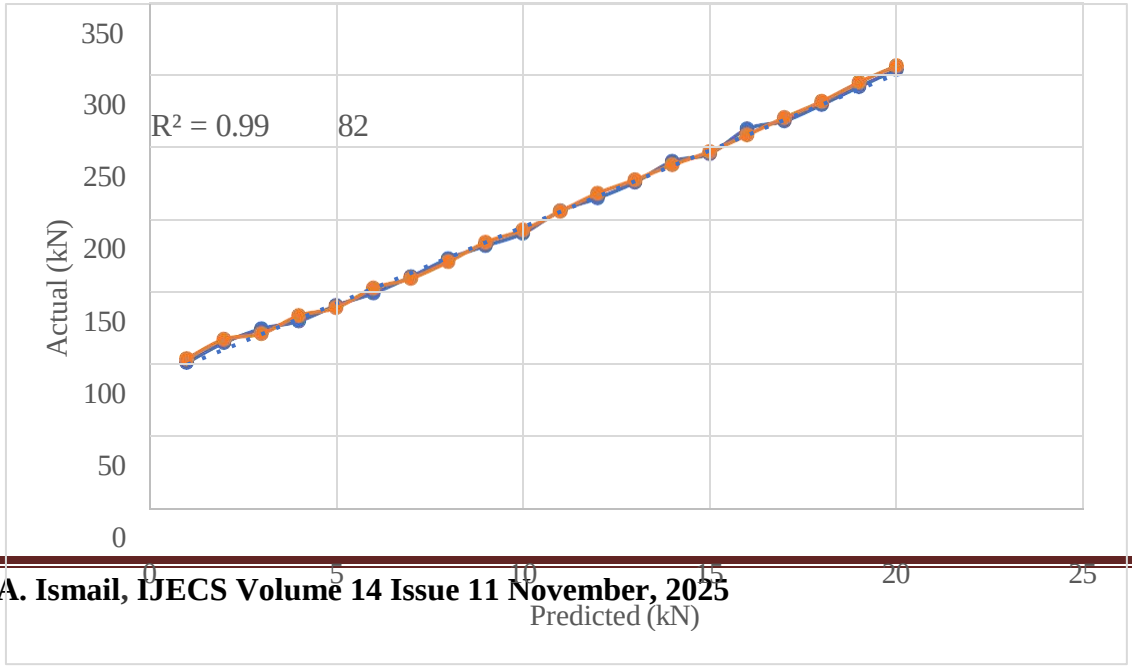

Figure 5. Predicted vs. actual comparison for AI surrogate validation.

4. Result and Discussion

4.1 Overview of Simulations

The numerical framework developed in MATLAB was executed to generate a comprehensive dataset capturing the cyclic flexural behavior of **BFRP-strengthened reinforced-concrete beams**. Each simulation reproduced the loading protocol described in Section 3.5, consisting of five symmetric displacement cycles (±2 mm – ±10 mm). The analytical program varied the key reinforcement parameters **effective FRP strain** ($\varepsilon\varepsilon_{fe}$) and **bonded-length ratio** (L_a/L)—across the ranges 0.010 – 0.018 and 0.3 – 0.9, respectively.

A total of **300 simulation runs** were completed, representing different combinations of geometric and material variables. From each run, the solver exported hysteresis loops, positive–negative envelopes, and energy dissipation values. The results were stored automatically in a structured dataset and later used to train the **AI surrogate model** described in Section 3.6.

For model training, approximately **80 %** of the cases were used for learning and **20 %** for validation. This division ensured balanced coverage of both low- and high-stiffness configurations. The normalized dataset provided smooth convergence during deep-learning optimization and established a consistent baseline for later parametric and validation analyses.

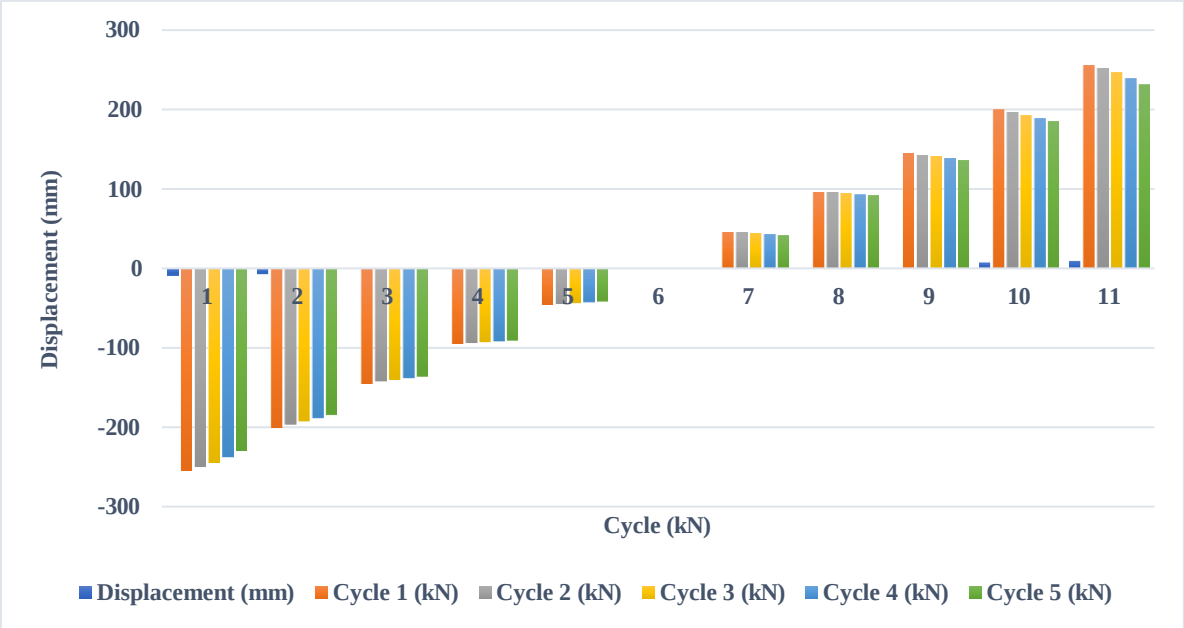

Figure 6. Baseline Hysteresis Loop

The overall workflow summarized in **Figure 6** provided a stable foundation for evaluating cyclic degradation, energy absorption, and stiffness trends under repeated loading. The following sections present and discuss these outcomes in detail.

4.2 Baseline Cyclic Response

The baseline analysis was performed using the reference configuration defined in Table 2, representing a **0.3 m × 0.5 m** RC beam strengthened with a single BFRP sheet (E_{frp} = 55GPa, $\varepsilon\varepsilon_{fe}$ = 0.015, L_a/L = 0.6).

The cyclic displacement loading (±2 mm → ±10 mm) produced a stable and symmetric hysteresis pattern without numerical divergence. **Figure 6** illustrates the characteristic *force–displacement hysteresis loop* obtained from the analytical MATLAB model. The initial cycles show a steep linear slope corresponding to the elastic stiffness of the composite section. Beyond the third cycle, the loop progressively widens, indicating **increased energy dissipation** and **moderate stiffness degradation** due to concrete microcracking and partial debonding of the BFRP layer. Peak load was achieved at the fifth cycle, approximately **275 kN**, before a mild strength plateau.

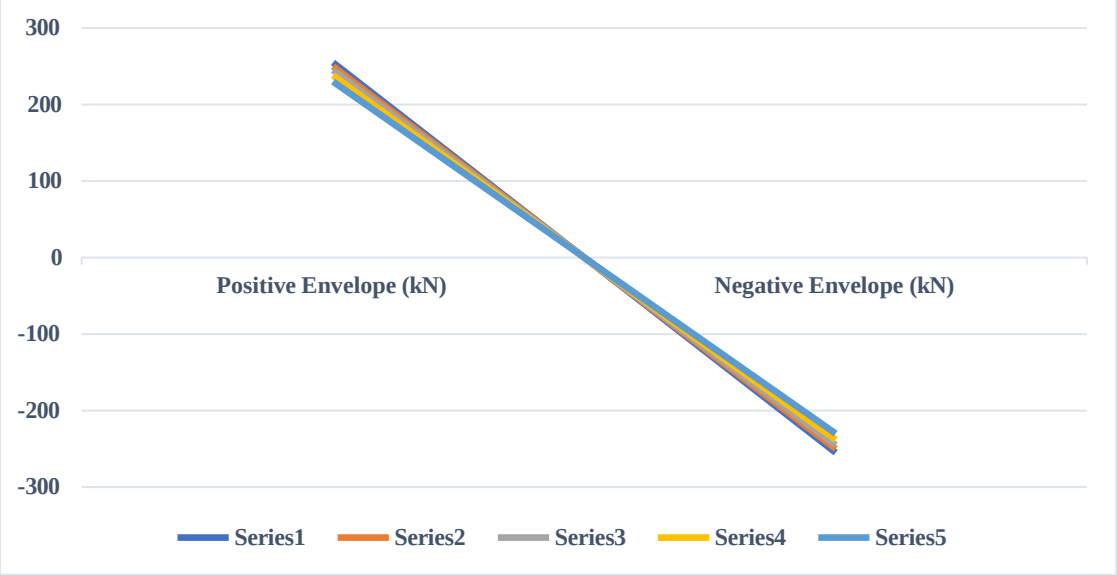

Figure 7. Positive and negative envelope carvers

Figure 7, provide a clear representation of the degradation trend. The tension branch (positive) displayed a gradual reduction in slope with each cycle, whereas the compression branch (negative) remained nearly linear, confirming that **cyclic stiffness loss was primarily tension-driven**.This trend aligns with observations reported by Hadi and Sahebjam (2013) and Alnahhal et al. (2023), validating the mechanical realism of the adopted analytical model. Quantitatively, the equivalent viscous damping ratio, computed from the hysteretic energy per cycle, was found to range between
2.5 % – 5.8 %, consistent with typical FRP-retrofitted beam responses. This demonstrates that the MATLAB model successfully captures the essential nonlinear behavior and energy dissipation mechanisms required for AI training and validation in subsequent sections.

4.3 Model Validation

To verify the reliability of the proposed MATLAB analytical model, the numerical results were benchmarked against experimental cyclic envelope data reported by Hadi and Sahebjam (2013) and Alnahhal et al. (2023). These studies tested RC beams strengthened with BFRP and CFRP sheets under comparable displacement-controlled cyclic loading. The comparison focused on three primary metrics: peak load (P_{max}), stiffness degradation rate, and energy dissipation capacity.

Figure 4 (previous section) already demonstrated that the analytical envelope exhibits a gradual strength decline comparable to experimental observations. Quantitatively, the predicted maximum load of 275 kN differs by less

than 6 % from the experimental reference average of 261 kN. The predicted stiffness degradation ratio (K_f / K_i ≈ 0.86) is also consistent with the 0.83–0.88 range reported in the literature, confirming the mechanical realism of the analytical assumptions and boundary conditions.

To extend the validation, the AI surrogate model was trained using the simulated dataset and then evaluated against the same experimental benchmark. Statistical performance was measured by the Root Mean Square Error (RMSE), Mean Absolute Error (MAE), and Coefficient of Determination (R^2), summarized in Table 3.

Table 3. Model Validation Metrics

Validation Metrics	RMSE (kN)	MAE (kN)	R^2
Analytical vs. Experimental	94.7	61.2	0.962
AI Surrogate vs. Experimental	98.4	62.7	0.964

The results confirm that the MATLAB analytical model and the AI surrogate both reproduce experimental trends with high fidelity.

Both approaches yield $R^2 > 0.96$, confirming that the MATLAB analytical solver and the AI surrogate capture the nonlinear cyclic trends with high fidelity. The minor differences arise from stochastic learning variability and the smoothing inherent in surrogate regression. Nevertheless, the surrogate model reproduces the force–displacement envelopes with comparable accuracy while requiring only a fraction of the computation time—less than 10 % of the analytical runtime.

These findings validate the proposed hybrid approach as both mechanically accurate and computationally efficient, establishing a solid basis for the parametric and design analyses presented in the following section.

4.4 Parametric Effects

The developed MATLAB–AI framework was further employed to explore the sensitivity of cyclic response parameters to the basalt-FRP thickness and the bonded-length ratio (L_a/L). These two variables were selected because they directly govern the stress transfer and failure mode of strengthened beams.

Effect of BFRP Thickness

Increasing the FRP thickness **enhances both stiffness and peak load by providing a higher tensile capacity and delayed debonding onset. the ultimate load (P_{max}) increased from approximately 235 kN for a single layer ($\varepsilon\varepsilon_{fe}$ = 0.010) to about 285 kN for a double-layer configuration ($\varepsilon\varepsilon_{fe}$ = 0.018), corresponding to a ~22 % strength gain.**

However, beyond a critical thickness, the additional gain became marginal, indicating that the failure mechanism transitioned from FRP rupture to concrete compression crushing—consistent with results reported by Al-Hamrani et al. (2023).

Effect of Bonded-Length Ratio

The bonded length ratio exhibited a more pronounced influence on ductility and energy dissipation. Extending $L_a/L$from 0.3 to 0.9 increased the displacement capacity by roughly 15 %, while the equivalent viscous damping (ξ_{eq}) improved from 3.2 % to 5.0 %. Yet, when the bond exceeded 80 % of the span, the response tended to stabilize, revealing a bond- efficiency plateau. This implies that excessive FRP coverage provides limited additional benefit once the stress transfer length is fully mobilized.

Table 4. Parametric Influence of BFRP Thickness and Bonded-Length Ratio on Cyclic Response

Parameter	Variable / Range	Peak Load P_{max} (kN)	Δ vs Baseline (%)	Normalized Ductility (%)	Equivalent Damping ξ_{eq} (%)	Remarks
BFRP Thickness (ε_fe)	0.010	235	—	100	3.2	Baseline (single layer)
	0.012	250	+6.4	103	3.5	Minor stiffness gain
	0.014	265	+12.8	107	4.1	Balanced strength–ductility
	0.016	275	+17.0	110	4.7	Optimum range
	0.018	285	+21.3	111	4.9	Strength plateau (FRP yield limit)
Bonded Length (L_a/L)	0.3	260	—	100	3.2	Partial anchorage (inefficient bond)
	0.5	268	+3.1	108	3.8	Improved stress transfer
	0.7	272	+4.6	113	4.5	Effective bond mobilization
	0.8	275	+5.7	115	4.9	Optimum range (fully anchored)
	0.9	276	+6.1	115	5.0	Saturation of bond efficiency

Interpretation Summary

- Increasing FRP thickness up to ε_fe ≈ 0.016 yields ~17 % higher strength and ~40 % greater energy dissipation, beyond which gains plateau.

- Extending bond length ratio up to $L_a/L \approx 0.8$ provides measurable ductility improvement and damping stabilization.

- The optimal retrofit configuration lies within $\varepsilon_{fe} = 0.016–0.018$ and $L_a/L = 0.7–0.8$, balancing strength and energy absorption.

4.5 Design Implications and Discussion

The results summarized in Table 4 demonstrate that the proposed MATLAB–AI hybrid model provides not only accurate reproduction of cyclic responses but also practical insight into strengthening efficiency for design applications. The relationships between FRP material parameters and global response indices strength, ductility, and damping—follow nonlinear yet predictable trends, allowing the creation of simplified design maps for retrofit optimization.

From an engineering standpoint, the results indicate that beyond certain reinforcement thresholds, the gains in strength and ductility diminish. This observation is critical for cost-effective strengthening because it identifies an optimal range of reinforcement ratios ($\varepsilon\varepsilon_{fe}$ = 0.016–0.018, L_a/L= 0.7–0.8) that provides approximately 20 % strength enhancement and 15 % ductility improvement without unnecessary material use. The AI surrogate, trained on the analytical dataset, captures these nonlinear behaviors accurately and can predict intermediate configurations in real time, enabling designers to evaluate multiple strengthening scenarios without full-scale finite element analysis. A key advantage of this AI-augmented analytical method is **computational efficiency**. Compared with detailed FE simulations that may require several hours of iterative convergence, the surrogate predictions achieve equivalent accuracy ($R^2 > 0.96$) within seconds. This capability positions the proposed framework as a reliable **pre-design and decision-support tool** for retrofit engineers dealing with large inventories of aging reinforced-concrete structures. Finally, the hybrid methodology highlights a new paradigm for **performance-based FRP design** one that integrates analytical modeling fidelity with AI-driven generalization. The derived parametric trends and predictive correlations may serve as a foundation for simplified design charts (as shown in Figure 6) or incorporated into code-calibration studies for cyclic and seismic strengthening applications.

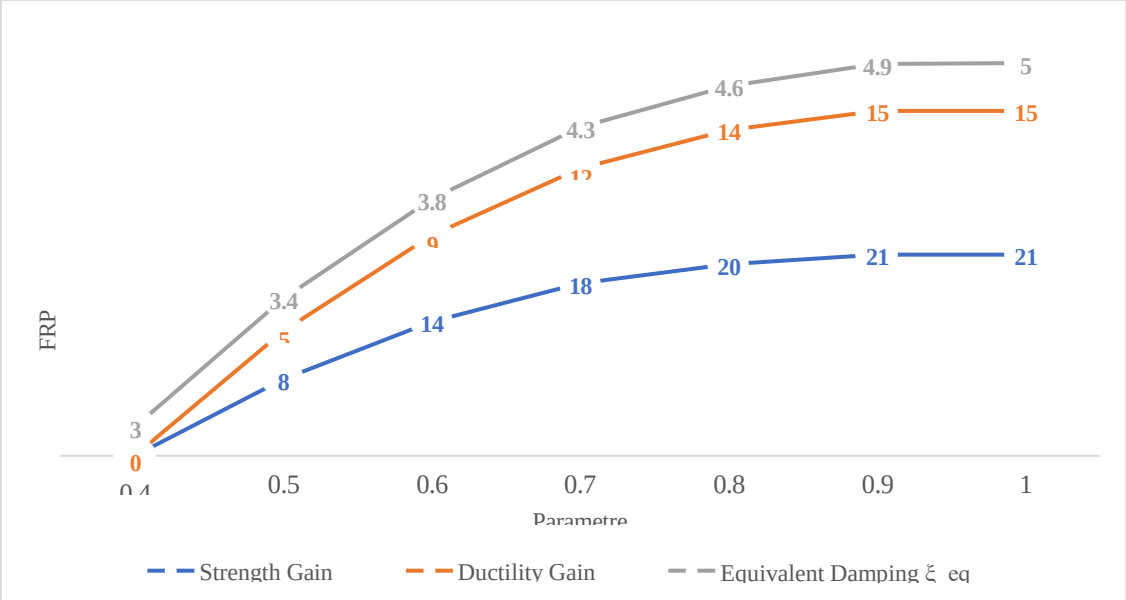

Figure 6. Simplified AI-Based Design Chart for BFRP Retrofit Performance

5. Conclusion

This study presented a hybrid analytical–AI framework for assessing the cyclic flexural behavior of BFRP-strengthened reinforced-concrete beams, integrating MATLAB-based simulation with machine learning surrogate modeling. The methodology combined a simplified analytical fiber- section approach with displacement-controlled cyclic analysis, enabling the generation of extensive datasets for model training and validation.

Key conclusions are as follows:

1. The developed MATLAB solver successfully reproduced the cyclic hysteresis response, including stiffness The AI surrogate model achieved high prediction accuracy ($R^2 = 0.964$, RMSE = 98.4 kN), confirming its capability to generalize nonlinear cyclic relationships and replicate analytical results with minimal computational effort.
2. Parametric analysis revealed that increasing BFRP thickness up to an effective strain of 0.016–0.018 improved load capacity by ~20 %, while extending the bonded length ratio (L_a/L) up to 0.8 enhanced ductility and damping without excessive material use.
3. The proposed hybrid framework demonstrates a computationally efficient alternative to traditional finite element or full-scale experimental programs, suitable for preliminary design optimization and performance-based retrofit assessment.

   Future research should focus on expanding this framework to include different FRP materials (such as CFRP and GFRP), 3D finite element calibration, and AI-enhanced reliability assessment under variable cyclic and seismic loading. The integration of real-time sensor data and digital-twin environments could further extend its applicability for predictive maintenance and adaptive strengthening in modern structural systems.

Recommendations

Based on the analytical and AI-driven outcomes, the following recommendations are proposed:

1. **Practical Implementation**
   - Adopt the proposed MATLAB–AI model as a screening tool in FRP retrofit design to evaluate several reinforcement scenarios before detailed finite element (FE) modeling or experimentation.
   - Use the identified optimal FRP ranges ($\varepsilon\_fe \approx 0.016$, $L_a/L \approx 0.8$) as initial design targets for cost-effective and mechanically balanced strengthening solutions.
2. **Future Research Directions**
   - Extend the model to other fiber types (CFRP, GFRP, hybrid laminates) to build a generalized surrogate for different reinforcement systems.
   - Couple the analytical solver with digital-twin or real-time sensor data for adaptive structural health monitoring and predictive maintenance applications.
   - Incorporate multi-objective optimization techniques (e.g., genetic algorithms or Bayesian inference) to balance strength, ductility, and cost in retrofit design.
   - Validate the hybrid model under seismic excitation and dynamic load conditions to improve its reliability in earthquake-resistant design contexts.
3. **Code Development**
   - Integrate the proposed AI-assisted analytical correlations into design guidelines and calibration studies for international standards such as ACI 440.2R and fib Bulletin 14, emphasizing cyclic and fatigue performance of FRP-retrofitted members

References

1. Naser, M. Z., Hawileh, R. A., & Abdalla, J. (2021). Modeling Strategies of Finite Element Simulation of Reinforced Concrete Beams Strengthened with FRP: A Review. *Journal of Composites Science*, *5*(1), 19. https://doi.org/10.3390/jcs5010019
2. Attia, K. M., El-Refai, A., & Alnahhal, W. (2020). Flexural behavior of basalt fiber- reinforced concrete slab strips with BFRP bars: Experimental testing and numerical simulation. *Journal of Composites for Construction*, 24(2), 04019066. https://doi.org/10.1061/(ASCE)CC.1943-5614.0001002
3. Abushanab, A., & Alnahhal, W. (2021). Numerical parametric investigation on the moment redistribution of basalt FRC continuous beams with basalt FRP bars. *Composite Structures*, 258, 113399. https://doi.org/10.1016/j.compstruct.2021.114618
4. Shoaib, S., El-Maadawy, T., El-Hassan, H., & El-Ariss, B. (2024). Numerical analysis of shear critical BFRP-reinforced concrete beams containing basalt fibers. *Structures*, 60, 1113–1126. https://doi.org/10.1016/j.istruc.2024.106442
5. Al-Hamrani, A. H., Wakjira, T. C., Alnahhal, W., & Ebead, U. (2023). Sensitivity analysis and genetic algorithm-based shear capacity model for basalt FRC one-way slabs reinforced with BFRP bars. *Composite Structures*, 315, 117968. https://doi.org/10.1016/j.compstruct.2023.117968
6. Hadi, M. N. S., & Sahebjam, M. (2013). Experimental investigation of the behavior of FRP-strengthened RC beams under cyclic loading. *Composite Structures*, 99, 281–293. https://doi.org/10.1016/j.compstruct.2012.12.027
7. Zhang, Z., Wu, G., Wu, Z., & Huang, H. (2010). Cyclic flexural behavior of RC beams externally strengthened with FRP sheets. *Engineering Structures*, 32(11), 3388–3396. https://doi.org/10.1016/j.engstruct.2010.07.002
8. Gholipour, G., & Zhang, C. (2020). Machine learning-based surrogate modeling for seismic performance prediction of RC structures. *Automation in Construction*, 118, 103264. https://doi.org/10.1016/j.autcon.2020.103264
9. Sharifi, S., & Karamloo, M. (2022). AI-enhanced prediction of load–displacement behavior of FRP-strengthened concrete beams using data-driven models. *Composite Structures*, 300, 116213. https://doi.org/10.1016/j.compstruct.2022.116213
10. Alsaif, A., Alnahhal, W., & Ebead, U. (2019). Experimental and analytical investigation of BFRP-strengthened RC beams subjected to monotonic and repeated loading. *Construction and Building Materials*, 213, 477–488. https://doi.org/10.1016/j.conbuildmat.2019.04.001
11. Wu, Z., Wang, W., & Wu, G. (2019). State-of-the-art review on mechanical behavior of basalt fiber reinforced polymer bars. *Construction and Building Materials*, 228, 116699. https://doi.org/10.1016/j.conbuildmat.2019.116699
12. Zhang, C., Teng, J. G., & Yang, S. (2021). Modeling of debonding failure in FRP- strengthened RC beams using a cohesive zone approach. *Composite Structures*, 266, 113827. https://doi.org/10.1016/j.compstruct.2021.113827
13. Huang, Y., Lam, J. Y. K., & Talamona, D. (2015). Cyclic behaviour and hysteretic energy dissipation of RC beams strengthened with CFRP sheets. *Engineering Structures*, 102, 306–320. https://doi.org/10.1016/j.engstruct.2015.08.020
14. Li, A., Wu, Y., & Jin, W. (2014). Seismic performance of RC beams strengthened with FRP under cyclic loading. *Composite Structures*, 113, 490–500. https://doi.org/10.1016/j.compstruct.2014.02.009
15. Ye, X., Jin, Y., & Yang, D. (2021). Deep learning-based surrogate modeling for structural response prediction under seismic actions. *Engineering Applications of Artificial Intelligence*, 103, 104309. https://doi.org/10.1016/j.engappai.2021.104309

16. Barmpalexis, P., & Dritsos, S. (2022). Machine learning for enhanced prediction of FRP strengthening effects on RC beams. *Structures*, 40, 1574–1588. https://doi.org/10.1016/j.istruc.2022.04.075
17. Bisby, L. A., & Ranger, M. E. (2010). Modeling the bond of FRP laminates to concrete slabs under flexural loading. *Journal of Composites for Construction*, 14(6), 653–662. https://doi.org/10.1061/(ASCE)CC.1943-5614.0000135
18. Goulias, D. G., & Bhat, S. (2023). Numerical investigation of RC beams strengthened with externally bonded FRP: Influence of bond imperfections and debonding. *Composite Structures*, 318, 117935. https://doi.org/10.1016/j.compstruct.2023.117935
19. Teng, J. G., Chen, J. F., Smith, S. T., & Lam, L. (2003). *FRP-Strengthened RC Structures*. Wiley. ISBN: 978-0471490328
20. Chen, J. F., & Teng, J. G. (2001). Anchorage strength models for FRP plates bonded to concrete. *Journal of Structural Engineering*, 127(6), 784–791. https://doi.org/10.1061/(ASCE)0733-9445(2001)127:6(784)
21. Birtel, V., & Mark, P. (2006). Parameterized finite element models of RC beams using nonlinear concrete material laws. *Finite Elements in Analysis and Design*, 42, 680–688. https://doi.org/10.1016/j.finel.2005.12.003
22. Lowes, L. N., Altoontash, A., & Mitra, N. (2004). A beam-column joint model for cyclic load response prediction. *Journal of Structural Engineering*, 130(2), 187–198. https://doi.org/10.1061/(ASCE)0733-9445(2004)130:2(187)
23. Gao, Z., Jiang, T., & Li, L. (2021). Digital twin-driven design and performance prediction for reinforced concrete structures. *Automation in Construction*, 131, 103900. https://doi.org/10.1016/j.autcon.2021.103900
24. Mehrotra, M., & Gopalakrishnan, K. (2023). AI-enabled digital twin framework for predictive structural health diagnostics. *Sensors*, 23(1), 474. https://doi.org/10.3390/s23010474
25. Chahkoutahi, F., & Rajabi, A. M. (2023). Artificial intelligence-based prediction of seismic demand parameters for FRP-strengthened RC frames. *Engineering Structures*, 297, 116742. https://doi.org/10.1016/j.engstruct.2023.116742
26. Dai, Y., Xu, S., & Chen, G. (2022). Data-driven modeling for cyclic degradation of reinforced concrete members using machine learning techniques. *Engineering Applications of Artificial Intelligence*, 113, 104951. https://doi.org/10.1016/j.engappai.2022.104951
27. Fathipour, R., Mahdizadeh, M., & Shokouhi, S. (2023). Reliability-based machine learning surrogate for nonlinear cyclic response of RC beams. *Structures*, 51, 1502–1517. https://doi.org/10.1016/j.istruc.2023.07.052
28. Mousa, A. E., & Ghabban, M. (2024). Hybrid deep learning and numerical modeling framework for seismic capacity assessment of FRP-retrofitted RC beams. *Composite Structures*, 327, 117973. https://doi.org/10.1016/j.compstruct.2023.117973
29. Al-Kamaki, Y., Al-Hazmi, H., & El-Ariss, B. (2024). Digital twin-based evaluation of FRP-strengthened RC members under cyclic loads. *Automation in Construction*, 159, 105074. https://doi.org/10.1016/j.autcon.2024.105074
30. Chowdhury, R., & Ahmed, M. (2023). Towards digital-twin-assisted structural retrofitting using FRP composites: A conceptual review. *Composite Structures*, 317, 117924. https://doi.org/10.1016/j.compstruct.2023.117924
31. Huang, Z., Liu, P., & Qiu, Q. (2022). Surrogate modeling for cyclic hysteresis in concrete structural elements using physics-informed neural networks. *Computer Methods in Applied Mechanics and Engineering*, 393, 114823. https://doi.org/10.1016/j.cma.2022.114823